Parametric study of hydraulic performance of flow with helical cruciform fuel for LWRs

Hyeongi Moon[a], Minseop Song[a*]
[a]*Hanyang University, Nuclear Engineering, 222 Wangsimni Rd., Seoul, PA 04763*
[*]*Corresponding author: hysms@hanyang.ac.kr*

***Keywords 123:** HALEU, Helical Cruciform Metal Fuel, SMR, Pressure Drop

1. Introduction

Recent safety concerns have propelled the development of Small Modular Reactors (SMRs), and South Korea is developing an innovative SMR (i-SMR) that adopts an integrated pressurized water-cooled reactor (iPWR) design. However, due to economies of scale, SMRs tend to be less economical than traditional large PWRs, potentially compromising the low levelized cost of energy (LCOE) that is a benefit of nuclear power.

This necessitates a review of mature but overlooked technologies that could resolve the economic challenges of SMRs. This study focuses on the Helical Cruciform-shaped Fuel (HCF) concept, which originates the three-petal metallic fuel used in Russian icebreaker nuclear reactors[1]. The geometry of HCF, which features a four-petalled support in a square array fuel rod assembly with a helical twist, allows for self-mixing of the coolant and a higher heat transfer area-to-volume ratio without the need for spacer grids. High-assay low-enriched uranium (~20%) HCF, applicable to large LWR reactors and derived from Russian icebreaker experience, is being researched and slated for irradiation tests at the Idaho National Laboratory's Advanced Test Reactor for licensing[2].

This study conducts hydraulic research targeting HCF application in SMRs, considering that modern PWR-type SMRs like the i-SMR and Nuscale rely on natural circulation and are sensitive to the pressure drop in the core region. Hence, a sensitivity study on HCF's cross-sectional shape and helical pitch is critical. The study presents calculated pressure drop using computational fluid dynamics (CFD) with structured mesh. Additionally, it includes vortex visualization to further analyze fluid flow characteristics and identify areas of complex flow patterns within the system.

2. Methodologies

In CFD analysis, setting the turbulence model is important because it can affect pressure drop by influencing the calculated values of Reynolds stress[3]. In this study, the engineering practical RANS method was used. Commonly used turbulence models for RANS numerical analysis include ***k-ε***, ***k-ω***, and SST. The ***k-ε*** turbulence model [4] simulates turbulent behavior relatively accurately in free-flowing regions with small pressure gradients, but inaccurately estimates boundary layer separation in viscous sublayer regions. The ***k-ω*** turbulence model developed by Wilcox [5] accurately analyzes flow separation due to adverse pressure gradients, but is sensitive to free-flowing regions. Menter [6] proposed an SST turbulence model that combines the advantages of the ***k-ε*** and ***k-ω*** models. The study was conducted as part of a preliminary CFD study, using the SST ***k-ω*** model for its engineering speed and good convergence.

2.1 Analysis domain and mesh

The study conducted a computational fluid dynamics analysis on the bypass of a 2 × 2 HCF, and the analysis domain and boundary conditions are as shown in Fig. 1. The analysis was performed to a total height of 1.8288 meters due to constraints in computational resources. When L as the total length of the helix, which is 1.8288m, and P as the pitch of the helix, which is the axial length per one complete turn, β is defined as follows.

$$(1)\quad \beta = \frac{L}{P} * 4$$

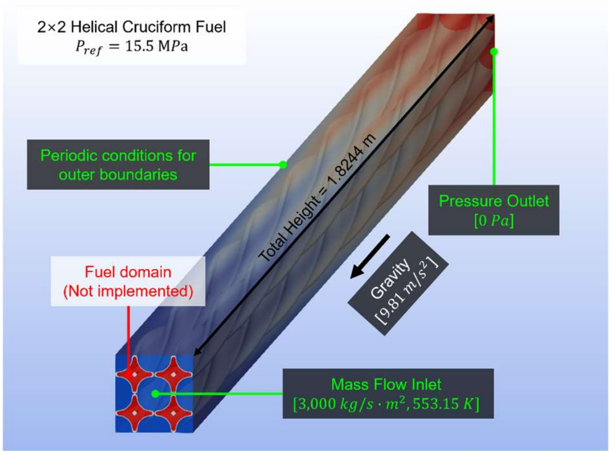

Fig. 1. Analysis domain for computational fluid dynamics.

The mesh was constructed using the open-source software Salome-9.9.0 based on Python 3 [7]. The shape, design parameters, and mesh of the analysis domain can all be found in Fig. 2. The Reynolds number of subchannel coolant is calculated as 334,267 when β is 12 and R_{valley} is 4.65mm

The fluid region's mesh was created using a total of 2.8 million structured (hexahedral) grids, ensuring that each cell directly contacts its adjacent cells face to face. The fluid area was divided into an inner fluid region and an outer fluid region to increase mesh quality. In addition, a sufficiently dense and thin grid was distributed near the wall surface to increase the reliability of the calculation for the boundary layer. The mesh of the displacer-fuel-cladding was not formed and considered in this study.

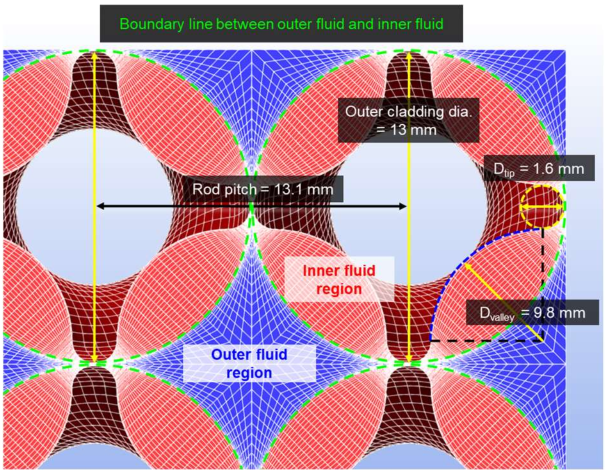

Fig. 2. Bottom view of the hexahedral mesh of the fluid domain (β = 12, R_{valley} = 4.65mm).

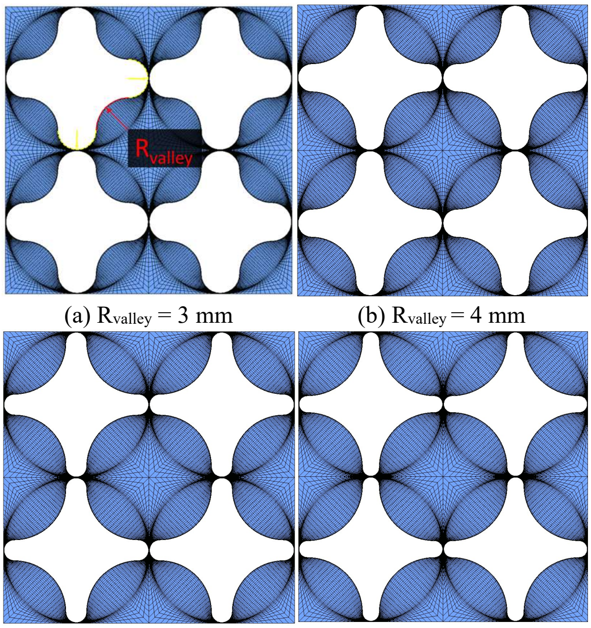

(a) R_{valley} = 3 mm (b) R_{valley} = 4 mm

(c) R_{valley} = 4.65 mm (d) R_{valley} = 5 mm

Fig. 3. Radius values of valley and corresponding mesh structures.

2.2 Parametric study set-up and solver settings

In this study, a sensitivity analysis was conducted on two parameters: the radius of the HCF's valley portion and β. Fig. 3 illustrates the shape of the fuel rod and the corresponding fluid section mesh according to R_{valley}. These meshes were automatically generated for various design parameters via python scripts, ensuring grid quality remains unaffected by changes in shape variables.

The solver settings are detailed in Table I, and the study utilized the Ansys CFX 2021 R2 version, a commercial CFD tool.

Table I: Solver settings

CFD tool	Ansys CFX
Heat transfer model	Total energy
Turbulence model	SST k-w
Interface model	GGI
Boundary walls	Periodic boundary condition
Advection scheme	High resolution
Turbulence numeric	High resolution

3. Results

3.1 CFD analysis results

While the verification of CFD results against reality is important, it is also crucial to assess whether the grid is sufficiently fine and whether the calculations have converged well. The results of the grid sensitivity study are shown in Fig. 4, where the velocity distribution along a line perpendicular to the height direction in the middle of the calculation domain was compared. Since there was no significant difference between the results from the fine grid and the very fine grid, all calculations were carried out using the fine grid. Fig. 5 demonstrates the convergence of the calculations, monitoring the velocity of points at the center of the calculation domain by advancing beta. It was confirmed that the velocity at all monitoring points converged well with iteration. For all analysis grids, y+ was calculated not to exceed 3.

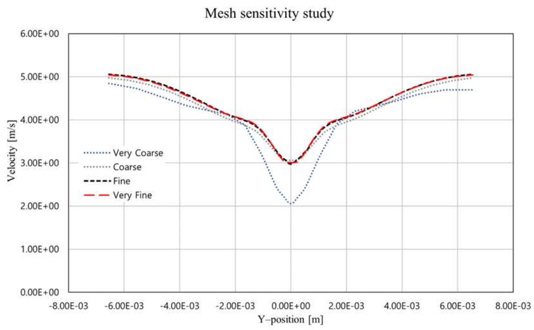

Fig. 4. Mesh sensitivity study results

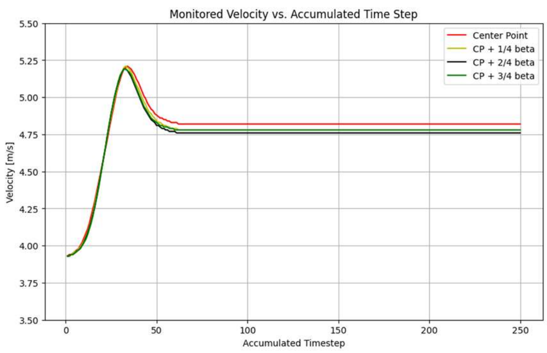

Fig. 5. Convergence of the velocity field at monitoring points.

This section briefly outlines key CFD analysis results, focusing on pressure drop, as illustrated in Fig. 2 and 3. The baseline geometry and boundary conditions derive from Deng et al. (2019)'s work, adopting a 0.9144m 360-degree twist height, which means $\beta = 8$ [8]. This study's HCF design parameters are similar to Lightbridge's HCF designs for PWR systems.

The parameter β, indicating the level of twist, positively affects heat transfer by enlarging the surface area. However, excessively increasing β leads to more rotations for fluid moving axially in the inner fluid region, increasing the effective travel distance to the core exit and thus raising the pressure drop.

With a fixed rod pitch, an increase in R_{valley} enhances the hydraulic diameter, as seen in Fig. 3, suggesting a potential reduction in pressure drop unless there's separated flow.

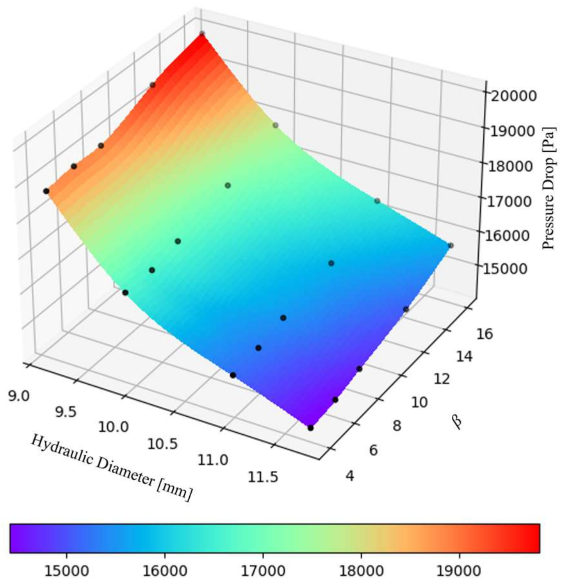

Fig. 6. Pressure drop as influenced by parametric variations in β and hydraulic diameter (cubic interpolated).

Table II: Pressure drop of parametric study results.

ΔP [kPa]		β				
		4	6	8	12	16
R_{valley} [mm]	3	18.8	18.9	18.9	19.5	19.9
	4	16.6	16.6	16.8	17.2	17.8
	4.65	15.2	15.3	15.5	15.8	16.4
	5	14.4	14.5	14.7	15.1	15.7

Table III: friction factor of parametric study results.

friction factor		β				
		4	6	8	12	16
R_{valley} [mm]	3	0.0159	0.0160	0.0160	0.0165	0.0168
	4	0.0152	0.0152	0.0154	0.0158	0.0163
	4.65	0.0155	0.0156	0.0157	0.0161	0.0167
	5	0.0157	0.0158	0.0160	0.0164	0.0170

A CFD analysis for 5 values of β and 4 of R_{valley} was conducted, with results summarized in Table II and III. These results were analyzed for trends using cubic interpolation, depicted in Fig. 6.

Fig. 6 replaced R_{valley} with calculated hydraulic diameter as the variable, showing that both HCF and typical fuel rods exhibit an increase in pressure drop with a decrease in hydraulic diameter and an increase in β.

Fig. 7 displays the pressure drop across typical fuel rod heights with the same hydraulic diameter as when R_{valley} is 4.65mm. The number of spacer grids in a typical Pressurized Water Reactor (PWR) is around 7 to 12 along the length of the fuel rods, and the APR1400 is designed to have 9 mid grids. For this, it was assumed that there are 4 spacer grids corresponding to the analysis height of 1.8288 m, and the pressure drop was calculated based on this assumption [9]. The pressure drop across the spacer grid has been sufficiently studied, and according to the research conducted by Wang et al (2022), it was simulated as 2,500Pa for each spacer grids [10].

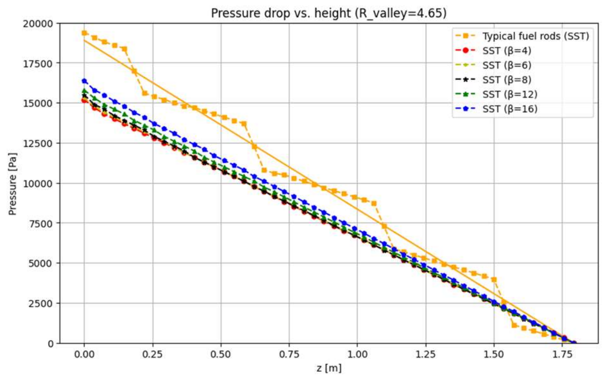

Fig. 7. Pressure drop vs height of HCFs and typical UO_2 cylinder fuel rods with spacer grids.

It was observed that as β increased to 4, 6, 8, 12, and 16, the pressure drop compared to traditional cylindrical fuel rods was respectively 80.4%, 81.0%, 81.8%, 83.8%, and 86.8%. Even in the most extremely twisted case of β is 16, it was possible to operate with a 13.2% reduction in pressure drop from the typical UO_2 fuel rods, affirming the hydraulic feasibility of applying this approach to SMRs.

2.4 Vortex core identification

Analyzing flow analysis results can enhance understanding of the flow by observing factors like vorticity, but it may be difficult to assess aspects such as flow stability. However, vortex core visualization allows for benefits in understanding flow dynamics, stability, and turbulence characteristics.

In this study, vortex core identification was performed using normalized helicity, which is defined as follows:

$$(2)\quad H_{normalized} = \frac{\vec{u}\cdot(\nabla\times\vec{u})}{|\vec{u}|\cdot|\nabla\times\vec{u}|}$$

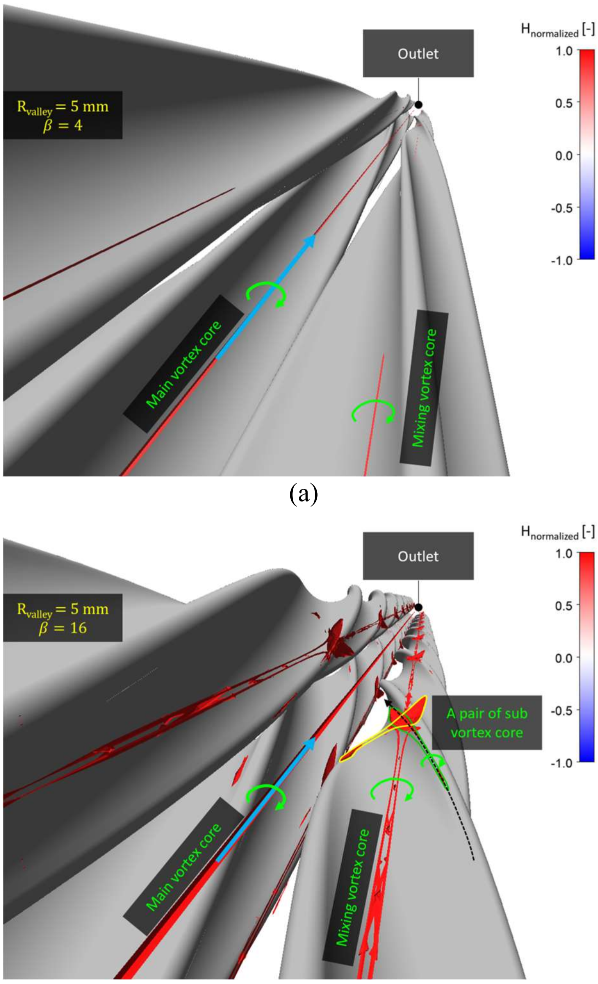

(b)

Fig. 8. the vortex core structures for two conditions: (a) when β equals 4 and (b) when β equals 16.

If the normalized helicity is 1, it means that the direction of flow matches the direction of rotation, and if it is -1, it signifies that the rotation is in the completely opposite direction. When the direction of flow and rotation match (the same for the negative direction), it indicates a highly coherent and stable vortex structure. In this analysis, negative normalized helicity values were calculated in the range of less than 0.2, and the primarily observed and identified vortex core is shown in Fig. 8.

For visibility, one HCF surface was hidden on the screen in the figure, and only cells with a normalized helicity of 1 were filtered for visualization. Fig. 8 (a) and (b) show cases with the same R_{valley} but different β values of 4 and 16, respectively. In the figure, with β = 4, the main vortex core, which continuously exists between four fuel rods, was defined. Additionally, a vortex core onset from the misalignment of rotational direction between fluid regions among two fuel rods was discovered, defined as the mixing vortex core. With β = 16, another distinctive pair of vortex cores was observed, defined as the sub vortex core. The sub vortex core occurs and disappears as the tips of two fuel rods come closer.

As β increases, the twist of the fuel also increases, resulting in more transverse flow and, consequently, a more developed vortical flow. Thus, the vortex cores observed at β = 16 were found to be thicker than those at β = 4. These results suggest that from the perspective of flow mixing, a lower β could reduce the mixing effect, and in terms of heat transfer, it gives us that modeling of heat transfer should not simply focus on surface area alone.

4. Conclusions

This study analyzed the hydrodynamic characteristics of the HCF. A sensitivity study of pressure drop with different geometries was conducted using the radius in the valley part and degree of twist as parameters. Within the analysis range, phenomena such as separated flow or secondary flow regions that interfere with the flow did not appear. It was confirmed that the pressure drop increases predictably as the hydraulic diameter decreases and the degree of rotation increases. Notably, the pressure drop notably increases when β increases from 8 to 12. Therefore, it seems hydraulically advantageous to set β below 12.

Moreover, vortex core identification was performed to enhance the understanding of flow characteristics. Visualization results were presented, taking into account the direction of vortex rotation through normalized helicity. It was observed that as β increases, the development degree of vortex cores increases. Only areas with a normalized helicity of 1 were filtered and shown. It was found that the normalized helicity of the flow rotating in the negative direction, i.e., the direction of rotation of the HCF's shape, does not develop significantly, reaching a maximum of about 0.2. In conclusion, as β increases, the influence of swirl flow becomes more pronounced. This will impact flow mixing and heat transfer aspects, thus requiring the selection of an appropriate β through thermal analysis.

However, for flows dominated by swirling flow, using a 2-equation model to solve them has accuracy limitations. Further analysis using higher-order turbulence models or methods less dependent on turbulence models may be required.

ACKNOWLEDGMENT

This work was supported by Korea Institute of Energy Technology Evaluation and Planning (KETEP) grant funded by the Korea government (MOTIE) (RS-2023-00243201, Global Talent Development project for Advanced SMR Core Computational Analysis Technology Development).

REFERENCES

[1] K. Shirvan, "Advanced LWR Fuel Designs with Significant Potential for Power Uprate", Presented at IAEA Technical Meeting on Light Water Reactor Fuel Enrichment beyond the 5% Limit: Perspectives and Challenges, Vienna, 12–16, 2015.

[2] NE-20.1-21540, Advanced Test Reactor Experiment Design for Measurement of Lightbridge Fuel™ Thermophysical Properties
[3] Q. Zhang, "Comparison on the thermal–hydraulic characteristics of wire-wrapped fuel and helical cruciform fuel by numerical simulation", Annals of Nuclear Energy, 2022.
[4] Brdina, J.E.; Huang, P.G.; Coakley, T.J. Turbulence modeling validation, testing and development. NASA Tech. Memo. 1997, 110446, 147.
[5] Wilcos, D.C. Re-assessment of the scale-determining equation for advanced turbulence models. AIAA J. 1988, 26, 1299–1310.
[6] Menter, F.R. Two-equation eddy-viscosity turbulence models for engineering applications. AIAA J. 1994, 32, 1598–1605.
[7] SALOME et al., SALOME - the open source integration platform for numerical simulation, 2019, CEA, EDF, Open Cascade
[8] Y. Deng, et al., Utilization of 3D fuel modeling capability of BISON to derive new insights in performance of advanced PWR fuel concepts, 2019, Journal of Nuclear Materials, Volume 516, 271-288
[9] US NRC document APR1400-Z-M-NR-14040-NP, ML15008A447, Structural Analysis of Fuel Assemblies for Seismic and Loss of Coolant Accident Loading, Rev.0, KHNP,(2014) 28-34
[10] X. Wang, Yingwen Liu, "The effects of spacer grid arrangement on flow boiling characteristics and critical heat flux in a complex 5 × 5 rod bundle channel", Case Studies in Thermal Engineering, 2022.